

Simulation of adsorbate-induced faceting on curved surfaces.

Daniel Niewieczerzał and Czesław Oleksy*

Institute of Theoretical Physics, University of Wrocław, Plac Maksa Borny 9, 50-204 Wrocław, Poland

(Dated: February 8, 2019)

A simple solid-on-solid model, proposed earlier to describe overlayer-induced faceting of bcc(111) surface, is applied to faceting of spherical surfaces covered by adsorbate monolayer. Monte Carlo simulation results show that morphology of faceted surface depends on annealing temperature. At initial stage surface around the [111] pole consists of 3-sided pyramids and step-like facets, then step-like facets dominate and their number decreases with temperature, finally a single big pyramid is formed. It is shown that there is reversible phase transition at which faceted surface transforms to almost spherical one. It is found that temperature of this phase transition is an increasing function of surface curvature. Simulation results show that measurements of high temperature properties performed directly and after fast cooling to low temperature lead to different results.

PACS numbers: 68.35.Rh, 68.43.De, 64.60.Cn, 68.35.Bs, 68.60.Dv

I. INTRODUCTION

It has been recently demonstrated that ultrathin metal films induce faceting of bcc(111) surfaces. Atomically rough W(111) and Mo(111) surfaces, when covered by a single physical monolayer of certain metals (Pd, Rh, Ir, Pt, Au) and annealed to $T > 700K$, undergo massive reconstruction from planar morphology to microscopically faceted surface^{1,2,3,4,5,6,7}. In most of investigated bcc(111) surfaces, the faceted morphology comprises 3-sided pyramids having {211} facets and facet sizes range from ~ 3 to 100 nm. It has been shown that metal that induces faceting acts like surfactant and remains on the surface during the faceting transformation⁷.

Suggestions that faceting in these systems is thermodynamically favorable have been confirmed by first-principles calculations^{7,8,9} performed for (111), (211), and (110) surfaces of Mo and W. Results show lowering of the surface energy when surfaces are covered by metal overlayer (e.g. Pd, Pt, Au). Moreover, at coverage of one physical monolayer, bcc(111) surface becomes unstable against faceting, i.e. system gains energy by transition from (111) to {211} orientation.

Interesting results have been obtained for faceting on curved surfaces of W and Mo in FIM (field ion microscopy) experiments^{10,11,12} and FEM (field emission microscopy) experiments^{13,14,15}. Initially spherical surface comprises macroscopic crystal facets. After deposition of metal (e.g. Pd, Pt) film or oxygen layer and annealing at elevated temperatures, increase of macroscopic {110} and {211} crystal facets is observed. An unexpected change in faceted morphology occurs near <111> poles where step-like {211} microfacets are formed^{10,11}. The number of step-like facets decreases with annealing temperature, and in some cases, a single {211} pyramid around the [111] pole is observed¹¹. Moreover, occur-

rence of new facets {123}, {178} in Pt on W and Pd on Mo has been reported in papers on FEM^{14,15}.

In theoretical studies of complicated surface problems (e.g. roughening transition, surface reconstruction, surface growth, surface phase transitions) simple models like lattice gas models or solid-on-solid (SOS) models are applied^{16,17,18,19,20,21,22,23}. In our earlier paper²⁴ we have proposed a SOS model to study adsorbate-induced faceting of bcc(111) crystal surface at constant coverage. Monte Carlo simulation results show formation of pyramidal facets in accordance with experimental observations. Moreover, the model describes reversible phase transition from faceted surface to disordered (111) surface. Such phase transition has been found in Pd/Mo(111) system³. In this paper we are going to study faceting of curved bcc crystal surface by using the SOS model. We will focus on changes in surface morphology in the vicinity of [111] pole where step-like {211} facets were observed in FIM experiments. The paper is organized as follows. In Sec.II SOS model for curved surface of bcc crystal is described. Results of Monte Carlo simulations, including changes in surface morphology with increase of annealing temperature, reversible phase transition are presented in Sec.III.

II. THE SOS MODEL

To study adsorbate-induced faceting on spherical surface we use earlier defined solid-on-solid model to describe faceting of bcc(111) surface²⁴. Let us recall the main assumptions. Atoms along the closed packed direction [111] form columns which are represented in the SOS model by their positions on (111) plane, $i = (i_x, i_y)$, and heights, h_i . Column positions form the triangular lattice (see Fig. 1) which is obtained by projection of bcc crystal lattice on the (111) plane. Each column comprises substrate atoms and one adsorbate atom occupying the highest place. This means constant coverage equal to 1 physical monolayer. There is also restriction imposed on columns heights, nearest neighbour columns

*Corresponding author.

Electronic address: oleksy@ift.uni.wroc.pl

can have difference of heights equal to $\pm 1, \pm 2$. A surface atom represented in the model by (i_x, i_y, h_i) has position $(i_x a_x, i_y a_y, h_i a_z)$ in bcc crystal where a_z is a distance between neighbouring (111) layers ($a_z = a\sqrt{3}/6$) and a

is the lattice constant. The model Hamiltonian represents surface formation energy which depends on column heights h_i in the following form

$$H = \frac{1}{2} \sum_i \left\{ \sum_{j_1} [J_1 \delta(|h_i - h_{j_1}| - 1) + K_1 \delta(|h_i - h_{j_1}| - 2)] + \sum_{j_2} [2J_2 \delta(|h_i - h_{j_2}|) + (2J_2 + K_2) \delta(|h_i - h_{j_2}| - 3)] + J_2 \sum_{j_3} [\delta(|h_i - h_{j_3}| - 2) + \delta(|h_i - h_{j_3}| - 4)] \right\} + NJ_0, \quad (1)$$

where sums over j_1, j_2 , and j_3 denotes summing over first, second, and third neighbours of a column at site i . Model parameters J_0, J_1, J_2, K_1 , and K_2 can be expressed by interaction energies between substrate and adsorbate atoms (for details see²⁴).

A. Initial conditions for spherical surfaces

We assume that surface has initially spherical shape determined by the radius R and the angular radius θ (see Fig. 2). Integer value of column height, h_i , is chosen to minimize the deviation from the height of corresponding spherical point. Positions of columns on (111) plane form the circle of radius $R_x = R \sin \theta$. We choose fixed boundary conditions, i.e., outside the circle the columns

form (111) face and their heights are frozen. Such boundary conditions make calculations much easier because the number of interaction constants in Hamiltonian (1) can be reduced to one constant, as will be shown in what follows. It is worth noting that we can also study flat (111) surface by appropriate choice of initial column heights in the circle. In this way we can compare adsorbate-induced faceting of flat and curved surfaces²⁷ using the same conditions, i.e. annealing temperature, annealing Monte Carlo time, number of surface atoms and boundary conditions. The restriction imposed on columns heights of the nearest neighbours (see Sec. II) limits the angular radius to $\theta \leq 20^\circ$. An example of spherical surface with $\theta = 20^\circ$ is shown in Fig. 3 where (111) facet and {211} facets occur together with terraces. There are also smaller facets with higher Miller indices. It is worth noting that on all surface images in this paper, the color of surface atom represents the number of its nearest neighbours having smaller heights. Such representation allows easy to identify different facets, e.g. {110} facets are represented by value 3 and row, trough of {211} facets by 5,1, respectively. Investigation of faceting of curved tungsten induced by palladium¹⁰ has revealed that step-like microfacets are formed in (111) crystal zones. Hence the present model will be used to study faceting around the single [111] pole on spherical surface.

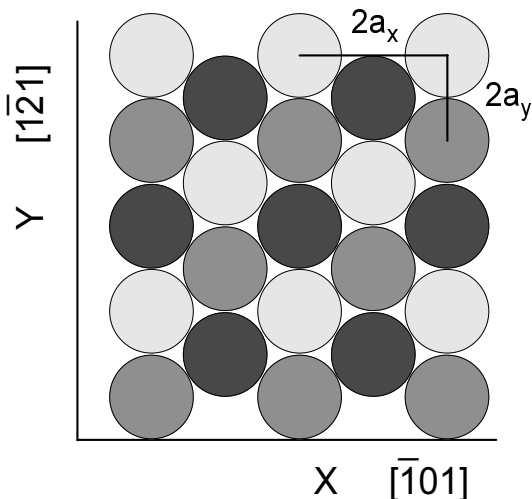


FIG. 1: Schematic top view of the bcc(111) surface. Atoms from three successive geometrical layers represent positions of columns in SOS model. The Z axis is normal to the (111) plane and $a_x = a\sqrt{2}/2$, $a_y = a\sqrt{6}/6$.

B. Energy of spherical surface

In the previous paper²⁴ it has been shown that energies per column of ideal faces (111), (211), and (110) are the same for the interactions limited to nearest neighbours. It turns out that the same is true for the energy of spherical surface. We calculated the number of bonds between nearest neighbours: b_1 with $|\Delta h| = 1$ and b_2 with $|\Delta h| = 2$ for hundreds of angles θ from the interval $[0^\circ, 20^\circ]$ and for constant number of columns N . For most of the angles, b_1 and b_2 are exactly the same as in the case of ideal (111) surface ($\theta = 0^\circ$). For a few angles b_1 and b_2 are a little changed e.g., $|\Delta b_1|/b_1 = 3.8 \times 10^{-4}$

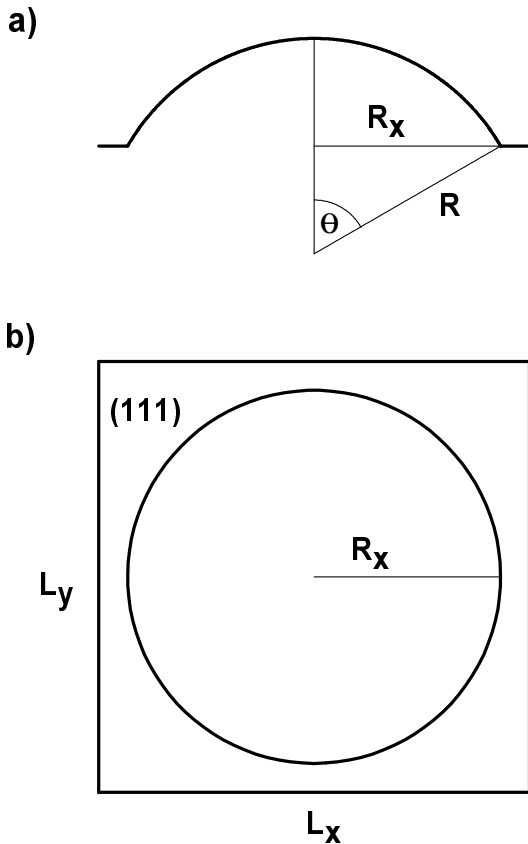


FIG. 2: Schematic (a) side view (b) top view of spherical surface.

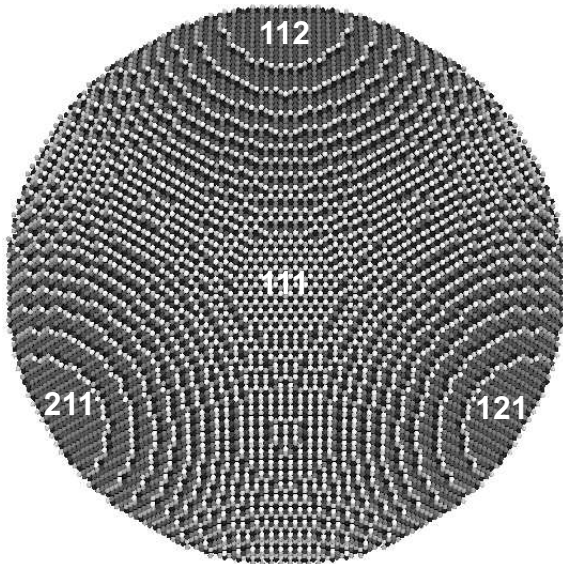


FIG. 3: Top view of spherical surface. Color of surface atom represents the number of its nearest neighbours (NN) having smaller heights. The brightest color is for 6 NN and the darkest one for 0 NN.

for $R_x = 93a_x$ ($N = 23497$) and $|\Delta b_1|/b_1 = 5.6 \times 10^{-5}$ for $R_x = 370a_x$ ($N = 327367$), and such angles will be omitted. On the other hand, permitted changes of a configuration do not change the number of bonds b_1 and b_2 . Thus energy of the nearest neighbours interactions is conserved in this SOS model and it can be neglected (or treated as reference energy). Due to this fact we can limit the number of model parameters to two (J_2, K_2). Similarly as in²⁴ we can eliminate one more parameter by choosing J_2 as the unit of energy. We will work with dimensionless quantities : energy $\tilde{H} = H/J_2$, temperature $\tilde{T} = k_B T/J_2$, and interaction constant $K = K_2/J_2$ (in what follows, the tilde will be omitted). It has been shown that energy of (211) face is minimal when $-2 < K < 0$ whereas (111) surface is stable for $K > 0$. Therefore simulation of flat SOS model²⁴ with negative K (e.g. $K = -1.25$) shows faceting of bcc(111) surface. In present model, energy of spherical surface E_{sp} decreases with θ for negative K but is still greater than energy of (211) face, e.g. energy per column for $K = -1.25$: $E_{111} = 7$, $E_{sp}(\theta = 20^\circ) = 6.26$ and $E_{211} = 5.75$. Thus we expect that spherical surface may undergo faceting after annealing at elevated temperature.

III. MONTE CARLO SIMULATIONS

Properties of the spherical SOS model with constant coverage are investigated by Monte Carlo (MC) simulation in canonical ensemble using standard Metropolis algorithm^{25,26}. A new configuration is generated by choosing two lattice sites i and j and changing heights of columns at these sites: $(h_i, h_j) \rightarrow (h_i - 3, h_j + 3)$. This is equivalent to moving a substrate atom from a site i to a site j . The new configuration is accepted with probability $p = \min(1, \exp(-\delta E/kT))$, where δE is the energy change of the system generated by transition to a new configuration. In simulation we measure typical quantities such as mean energy $\langle H \rangle$, heat capacity

$$C_V = (\langle H^2 \rangle - \langle H \rangle^2)/k_B T^2, \quad (2)$$

the square mean width of the surface,

$$\delta h^2 = \left\langle \frac{1}{Na^2} \sum_j (h_j - \langle h \rangle)^2 \right\rangle. \quad (3)$$

The latter quantity depends also on curvature radius, therefore we introduce the square radial deviation

$$\delta r^2 = \left\langle \frac{1}{Na^2} \sum_j (r_j - R)^2 \right\rangle \quad (4)$$

where r_j is distance of surface atom j from the center of the sphere.

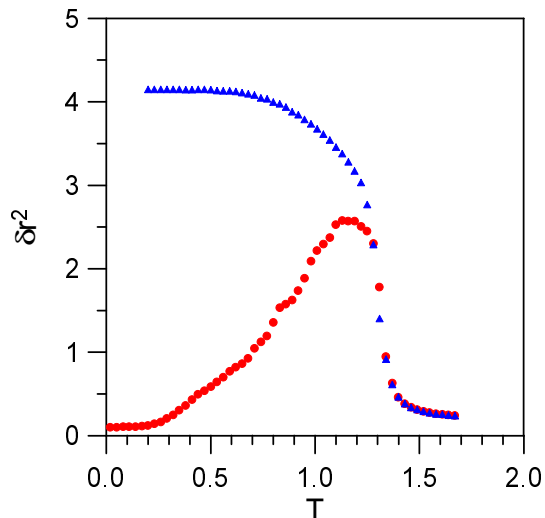


FIG. 4: Temperature dependence of δr^2 during the warming up (red circles) and the cooling down (blue triangles) the system.

A. Faceting of curved surfaces

In this section we investigate changes of surface covered by physical monolayer of adsorbate during the warming up and cooling down processes. Simulation starts at temperature T_0 , with spherical surface determined by the radius R and the angle θ (see section II A). Warming up process is characterized by gradual elevation of temperature, $T_i = T_{i-1} + \Delta T$. At each temperature system is annealed for time τ , measured in Monte Carlo steps per site (MCS). After reaching the maximal temperature, the system is cooling down by changing $\Delta T \rightarrow -\Delta T$. In order to measure temperature dependence of interesting quantities we choose 1000 of configurations in final stage at each temperature and we repeat warming up - cooling down cycle for 20 samples. In what follows we will explain why averaging over samples is important in this problem.

Results of simulations performed for the following parameters: $K = -1.25$, $R_x = 93a_x$, $\theta = 20^\circ$, $\Delta T = 0.03$ and $\tau = 2 \times 10^5$ are presented in Figs. 4 – 9. The temperature dependence of δr^2 in the warming up - cooling down cycle clearly shows (see Fig. 4) that this process is nonreversible. For $T > 0.3$ the square radial deviation increases as temperature is elevated which means that $\{211\}$ facets are formed on initially spherical surface. First we observe two types of facets on the surfaces (see Fig.5(a) and Fig.6): 3-sided pyramids and pits located near the pole and elongated facets forming steps between the $\{211\}$ faces. Steps are built of two alternating facets, e.g. (211) and (121). They have characteristic parallel long edges, oriented along $\langle 311 \rangle$ directions, which are seen in FIM experiments^{10,11} as bright lines. It is worth noting that there are also concave edges

(dark lines on Fig.6) which are not present in FIM images. Further increase of temperature causes disappearing of pyramids and reduction of the number of steps (see for example Fig.5(b)). In other words, a single pyramid with multiple edges is observed. As temperature is elevated the number of edges is reduced (see Fig.5(c)). In high enough temperature, it is possible to observe a single 3-sided pyramid on the surface (see Fig. 5(d)), sometimes a pyramid has a double edge. Above $T_d = 1.31$, a rapid decline of the δr^2 is observed. This means the defaceting transition at which pyramid disappears (see e.g. Fig.8(a)). Although δr^2 is very small above T_d , surface is not spherical. We observe also that the surface energy rapidly increases at T_d and heat capacity has maximum. A similar defaceting transition was obtained in simulation of faceting of bcc(111) surface²⁴ and observed in LEED experiment³ for Pd on Mo(111). The reverse process of slow cooling down the system from the highest temperature, leads again to faceting at the temperature T_d . Hence this is the reversible phase transition. However, in the cooling process a big single pyramid is formed on the surface just below T_d and the square radial deviation is going to maximal value as temperature decreases.

B. Measurements after fast cooling

In FIM experiment¹¹ the number of parallel edges on faceted curved surface was measured as function of annealed temperature. Because the FIM images are taken after rapid cooling to low temperature, we adopted a similar procedure to measure the average number of parallel edges, n_e . Configurations chosen at temperature T were quickly cooled down (system was held for 20 MCS at each T_i) to temperature $T_m = 0.2$ at which calculations were performed. Such procedure reduces thermal disorder and simple algorithm of searching edges could be applied. It is interesting to note that number of parallel edges decreases with temperature till defaceting temperature and then suddenly increases (see Fig.7). Similar behaviour was observed in FIM experiment¹¹. The reason why fast cooling can reproduce pyramid with multiple edges lays in morphology of disordered surface. When temperature is elevated over T_d the pyramid is initially damaged near the apex and along the edges. In these regions surface is not spherical but has disordered hill-and-valley structure, i.e. there are many of small $\{211\}$ facets which form irregular, short $\{211\}$ steps. As temperature is elevated the disordered regions broaden (see Fig.8(a)). On other hand, fast cooling causes return to pyramid with multiple edges (see Fig.8(b)) and multiplicity depends on width of disorder region and cooling speed. This fact can be used to estimate T_d from experimental results provided that obtained temperature is below desorption temperature. We have also checked how this effect depends on cooling speed. If the cooling is 10 times faster then this effect does not occur, i.e. the disorder surfaces is frozen for

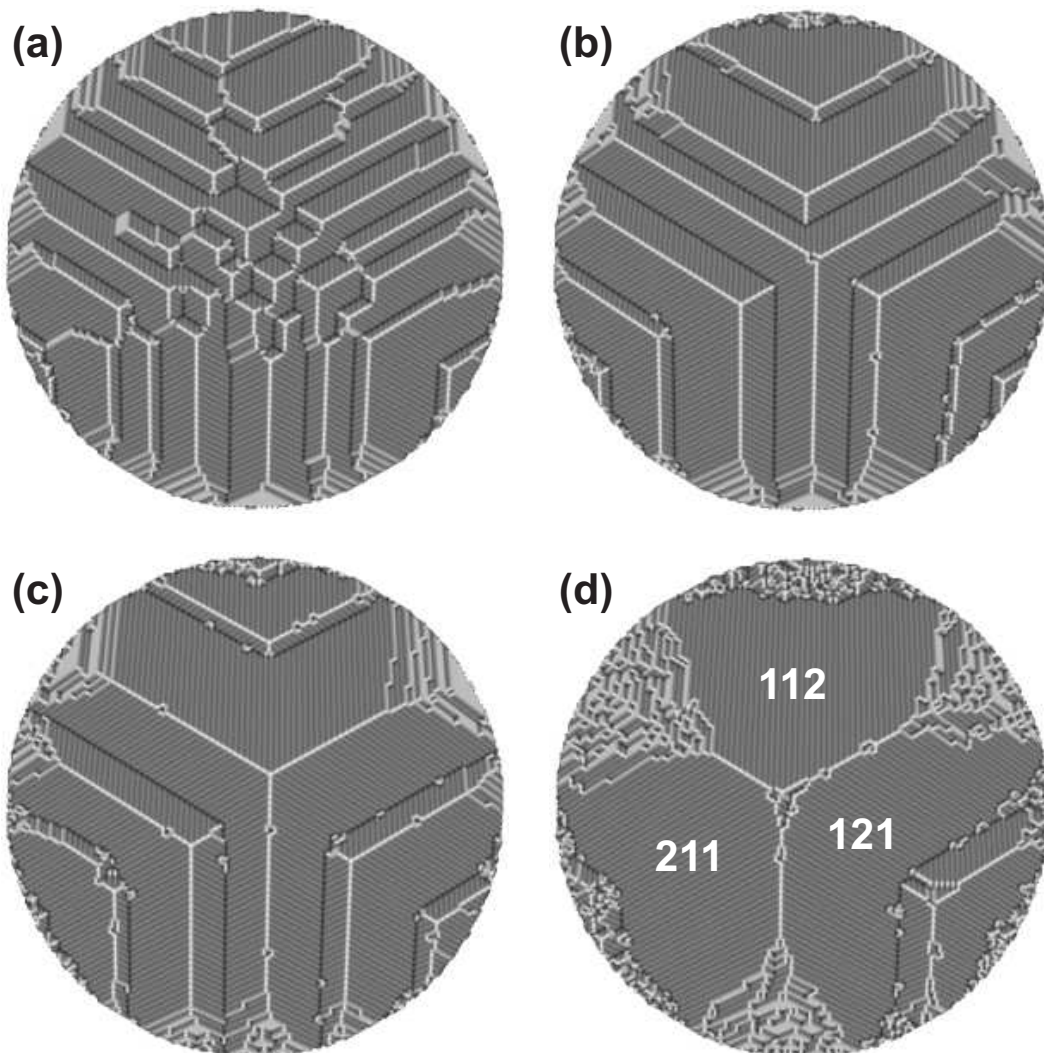


FIG. 5: Top view of the surface after annealing to: (a) $T = 0.41$, (b) $T = 0.68$, (c) $T = 0.86$ and (d) $T = 1.10$.

such cooling speed. On the other hand, cooling of the disordered phase will end up with a big 3-sided pyramid on the surface for speed of cooling over hundred times slower.

We observe that quantities like n_e , δr^2 , δh^2 have different temperature behaviour for a single sample and when they are averaged over many samples. The single sample temperature dependence of these quantities have step-like character (e.g. see Fig.9). We think that this effect is connected with large sizes of step-like $\{211\}$ facets on curved surface. A massive transport of atoms is needed to reduce one convex edge by merging two neighbouring $\{211\}$ steps. Of course, there should be an energetic barrier for such process and the barrier height depends on the size of $\{211\}$ facets. Therefore the width of plateau occurring in $n_e(T)$ on Fig.9 increases with annealing temperature. On the other hand, $n_e(T)$ averaged over many sample becomes a smooth function of temperature because facets growth proceeds in individual way for each sample due to the fact that distances between edges are

not constant at given T (see Fig.5) but they have visible dispersion.

C. Defaceting of curved surfaces

It has been mentioned in Sec III A that defaceting temperature, T_d , of spherical surface with ($\theta = 20^\circ$) is greater than in the case of planar surface. To investigate dependence of T_d on surface curvature we performed a series of simulations for several angles θ , keeping number of columns N (or R_x) constant. This means that the radius $R = R_x / \sin \theta$ of spherical surface was varied. Simulation started from high temperature and during cooling process with $\Delta T = 0.01$ we measured surface energy, heat capacity, square mean width and square radial deviation near the reversible phase transition. At each temperature system was held for 10^6 MCS. We see in Fig.10(a) that surface energy of flat surface rapidly decreases at

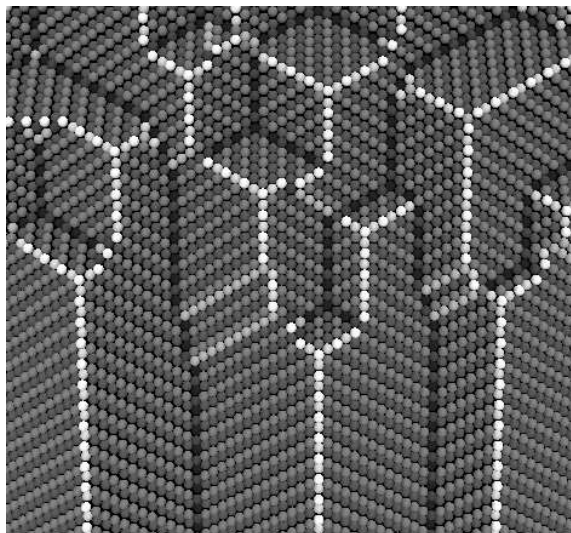


FIG. 6: Enlargement of a region from Fig.5(a) where step-like facets and pyramids (pits) coexist.

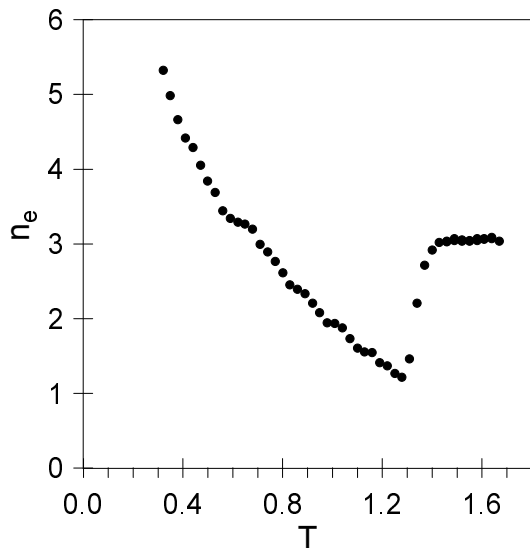


FIG. 7: Average number of parallel edges versus temperature calculated after fast cooling to $T = 0.2$.

defaceting temperature T_d . This is the first order phase transition and the energy difference is equal to the latent heat. However, temperature of defaceting increases as curvature of the surface increases. For surface with $\theta = 20^\circ$ the change of T_d is about 10% with respect to the flat case. We also see that change of the surface energy at phase transition decreases with θ . The same behaviour is observed in dependence of δh^2 on T and θ (see Fig.10(b)).

We think that increase of T_d with θ is connected with reduction of entropy in the disordered phase. The surface free energy (SFE), $F = E - TS$, of faceted phase F_f at the transition temperature T_d is equal to SFE of disordered

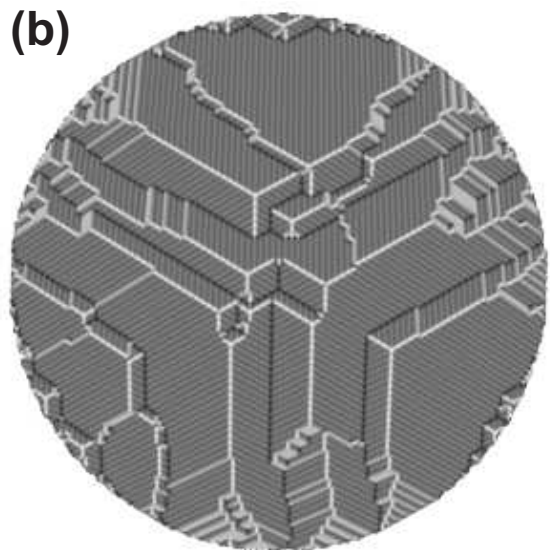
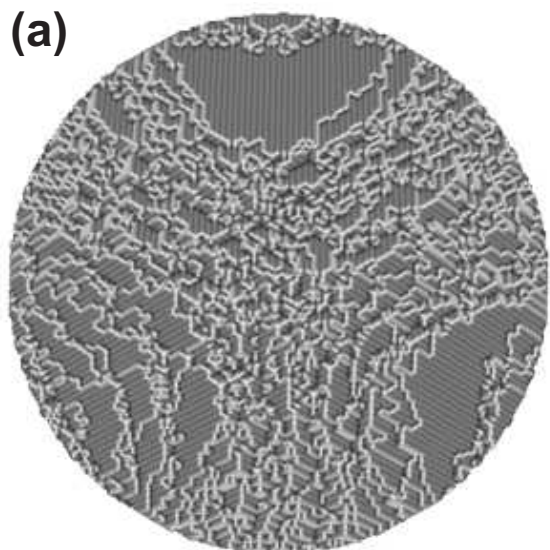


FIG. 8: Snapshot of the surface (a) at $T = 1.4$, (b) after fast cooling from $T = 1.4$ to $T = 0.2$.

phase F_d . Therefore temperature of phase transition can be obtained from $T_d(\theta) = \Delta E(\theta, T_d) / \Delta S(\theta, T_d)$ where $\Delta X = X_d - X_f$ for $X = E, S$. As is seen in Fig.10(a) the change of internal energy ΔE decreases with θ at T_d . Thus change of entropy ΔS should also be a decreasing function of θ . The decrease of entropy in disordered phase with θ can be justified by observed increase of $\{211\}$ areas and contraction of disordered regions on surface at T_d as curvature (or θ) increases.

IV. DISCUSSION

It is shown that a simple solid-on-solid model can be applied to study adsorbate-induced faceting of spherical

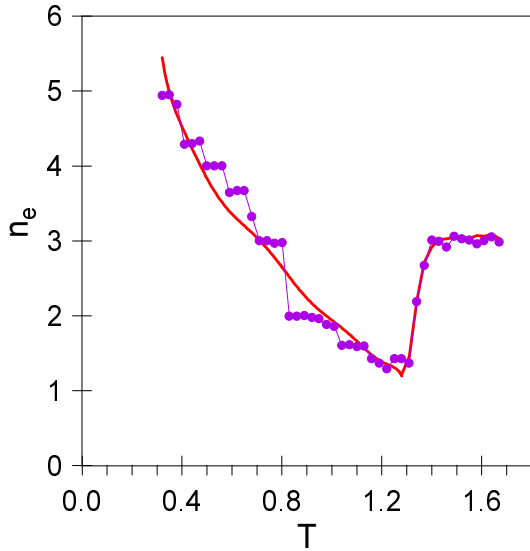


FIG. 9: Number of parallel edges for a single sample (circles) and averaged over 20 samples (thick line).

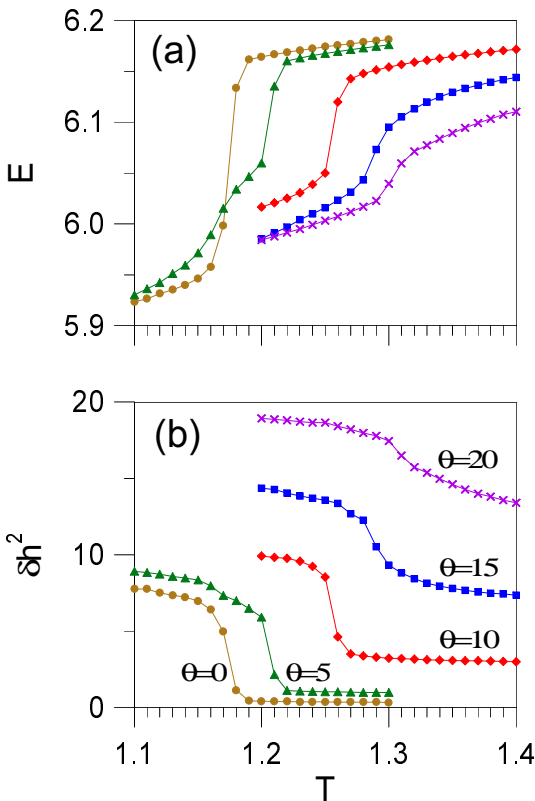


FIG. 10: Dependence of (a) surface energy, (b) square mean width on temperature near faceting - defaceting transition for several angles θ .

surface. Similarly as in the case of faceting of bcc(111) surface, it is possible to specify interaction constants to describe situation when initially prepared spherical surface covered by physical monolayer of adsorbate has surface formation energy greater than $\{211\}$ surfaces. Thus, the faceting of curved surface is thermodynamically favorable. Results of Monte Carlo simulations show that morphology of faceted surface depends on annealing temperature. One can distinguish three stages: (1) Formation of 3-sided pyramids around the $[111]$ pole and step-like $\{211\}$ facets between faces of $\{211\}$ orientations. The latter form long edges observed in FIM experiments^{10,11}. (2) Disappearing of pyramids around the $[111]$ pole and domination of step-like facets which number decreases with temperature. (3) Formation of a single big pyramid on the surface. It is worth noting that last two cases were described in papers on FIM experiments. The first case, mixture of two kind of facets has not been experimentally detected yet. We can investigate in detail structure of faceted spherical surface. In particular, properties difficult for experimental studies: concave edges between elongated facets, transition from step-like facets pyramids and pits, defects, etc.

It is shown that there is temperature of faceting - defaceting transition T_d above which disordered regions appear along pyramid edges. Although radial square deviation δr^2 rapidly declines above T_d , surface is not spherical. G. Antczak et al¹⁴ observed in FEM experiment of Pt on W tip emitter that faceting diminishes at $T > 1600K$ and hemispherical form of the emitter is recovered. As platinum is desorbed from tungsten emitter at temperatures above $1900K$ ¹⁴, this observation can indicate that defaceting occurs in Pt on W system. It would be interesting to verify experimentally this suggestion. We found that at temperatures just above T_d , disordered regions are not "spherical" but they have disordered hill-and valley structure with many small $\{211\}$ facets which form irregular short $\{211\}$ steps. This fact seems to be important for measurement of high temperature properties performed after fast cooling to low temperature, e.g. taking images in FIM experiments. It is shown that fast cooling may transform disordered surface into multi step surface (see Fig.8(b)). This is manifested in temperature behaviour of number of parallel edges n_e where unexpected increase begins above the phase transition temperature T_d (see Fig.7). Similar behaviour of n_e has been found for oxygen adsorbed on curved W¹¹. We think that this fact can be used to determine temperature of defaceting provided that T_d is below the desorption temperature (desorption is not included in the model). Formation of facets after rapid cooling of disordered surface can be explained by fast massive atomic rearrangement. Such effect has been observed in Pd/Mo(111) system³ in which 3-sided pyramidal facets occur on the bcc(111) surface after annealing to elevated temperatures. Above $T_d \approx 870K$ pyramids disappear and surface becomes planar. Attempts of freezing the high temperature planar phase ended up with faceted

surface even for 60 K/s of cooling rate.

Another interesting property of faceting found in MC simulation is dependence of T_d on surface curvature. Temperature of transition T_d on flat surface is smaller than T_d on curved surface. In FEM experiment¹⁴, faceting of Mo emitter covered by Pd has been observed in temperature range 750 – 1040K, so in temperatures above $T_d \approx 870K$ for Pd/Mo(111) system³. However, this can not be evidence of higher defaceting temperature in curved system because FEM observations were

made at room temperature and earlier discussed cooling effect could affect the FEM results.

Acknowledgements

We would like to thank dr Andrzej Szczepkowicz for discussions and help in preparing images.

-
- ¹ C.-Z. Dong, J. Guan, R. A. Campbell, T. E. Madey, in: X. Xie, S. Y. Tong, M. A. van Hove (Eds.), *The Structure of Surface IV*, World Scientific, Singapore, 1994, p. 328.
- ² C.-Z. Dong, L. Zhang, U. Diebold, T. E. Madey, *Surf. Sci.* 322 (1995) 221.
- ³ Ker-Jar Song, J. C. Lin, M. Y. Lai, Y. L. Wang, *Surf. Sci.* 327 (1995) 17.
- ⁴ T. E. Madey, J. Guan, C.-H. Nien, C.-Z. Dong, H.-S. Tao, R. A. Campbell, *Surf. Rev.Lett.* 3 (1996) 1315.
- ⁵ C.-H. Nien, T. E. Madey, *Surf. Sci.* 380 (1997) L527.
- ⁶ T. E. Madey, C.-H. Nien, K. Pelhos, J. J. Kolodziej, I. M. Abdelrehim, H.-S. Tao, *Surf. Sci.* 438 (1999) 191.
- ⁷ C.-H. Nien, T. E. Madey, Y. W. Tai, T. C. Leung, J. G. Che, C. T. Chan, *Phys. Rev. B* 59 (1999) 10335.
- ⁸ J. G. Che, C. T. Chan, C. H. Kuo, T. C. Leung, *Phys. Rev. Lett.* 79 (1997) 4230.
- ⁹ C. T. Chan, J. G. Che, T. C. Leung, *Progress in Surface Science* 59 (1998) 1.
- ¹⁰ A. Szczepkowicz, A. Ciszewski, *Surf. Sci.* 515 (2002) 441.
- ¹¹ A. Szczepkowicz, R. Bryl, *Surf. Sci.* 559 (2004) L169.
- ¹² A. Szczepkowicz, R. Bryl, *Phys. Rev. B* 71 (2005) 113416.
- ¹³ K. Pelhos, T. E. Madey, R. Błaszczyszyn, *Surf. Sci.* 426 (1999) 61.
- ¹⁴ G. Antczak, T. E. Madey, M. Błaszczyszyn, R. Błaszczyszyn, *Vacuum* 63 (2001) 43.
- ¹⁵ G. Antczak, R. Błaszczyszyn, T. E. Madey, *Prog. Surf. Sci.* 74 (2003) 81.
- ¹⁶ A.C. Levi, M. Kotrla, *J.Phys.: Condens. Matter* 9 (1997) 299.
- ¹⁷ K. Sasaki, *Surf. Sci.* 318 (1994) L1230.
- ¹⁸ H. van Beijeren, *Phys. Rev. Lett.* 38 (1977) 993.
- ¹⁹ G. Mazzeo, E. Carlon, H. van Beijeren, *Phys. Rev. Lett.* 74 (1995) 1391.
- ²⁰ S. Prestipino, G. Santoro, E. Tosatti, *Phys. Rev. Lett.* 75 (1995) 4468.
- ²¹ G. Santoro, M. Vendruscolo, S. Prestipino, E. Tosatti, *Phys. Rev. B* 53 (1996) 13169.
- ²² N.C. Bartelt, T.L. Einstein, E.D. Williams, *Surf. Sci.* 312 (1994) 411.
- ²³ V. P. Zhdanov, B. Kaseno, *Phys. Rev. B* 56 (1997) R10067.
- ²⁴ C. Oleksy, *Surf. Sci.* 549 (2004) 246.
- ²⁵ D.P. Landau, K. Binder, *A Guide to Monte Carlo Simulation in Statistical Physics*, Cambridge University Press (2000).
- ²⁶ K. Binder, D.W. Heermann, *Monte Carlo Simulation in Statistical Physics*, Springer-Verlag (Berlin, 1988).
- ²⁷ A. Szczepkowicz, A. Ciszewski, R. Bryl, C. Oleksy, C.-H. Nien, Q. Wu, and T. E. Madey, submitted to *Surface Science* (2005).